Analytical properties and optimization of time-delayed feedback control

K. Pyragas[1,2,*]

[1]*Max-Planck-Institut für Physik komplexer Systeme, Nöthnitzer Strasse 38, D01187 Dresden, Germany*
[2]*Semiconductor Physics Institute, LT-2600 Vilnius, Lithuania*

Time-delayed feedback control is an efficient method for stabilizing unstable periodic orbits of chaotic systems. If the equations governing the system dynamics are known, the success of the method can be predicted by a linear stability analysis of the desired orbit. Unfortunately, the usual procedures for evaluating the Floquet exponents of such systems are rather intricate. We show that the main stability properties of the system controlled by time-delayed feedback can be simply derived from a leading Floquet exponent defining the system behavior under proportional feedback control. Optimal parameters of the delayed feedback controller can be evaluated without an explicit integration of delay-differential equations. The method is valid for low-dimensional systems whose unstable periodic orbits are originated from a period doubling bifurcation and is demonstrated for the Rössler system and the Duffing oscillator.

I. INTRODUCTION

Ott, Grebogi, and Yorke [1] have suggested a method allowing a conversion of chaotic attractor to any of a large number of time periodic motions. The main idea relies on the fact that a chaotic attractor has typically embedded in it a dense set of unstable periodic orbits (UPOs) that can be stabilized by a small feedback perturbation. This idea stimulated a development of a rich variety of new chaos control techniques [2] among which the delayed feedback control (DFC) method [3] has become rather popular. The DFC is based on applying a feedback proportional to the deviation of the current state of the system from its state-one period in the past so that the control signal vanishes when the stabilization of the desired orbit is attained. The method has the advantage of not requiring prior knowledge of anything but the period of the desired orbit. It is particularly convenient for fast dynamical systems since it does not require the real-time computer processing. The time-delayed feedback control has been successfully used in quite diverse experimental contexts including electronic chaos oscillators [4], mechanical pendulums [5], lasers [6], a gas discharge system [7], a chaotic Taylor-Couette flow [8], chemical systems [9], and a cardiac system [10]. Socolar, Sukow, and Gauthier [11] improved an original DFC scheme by using an information from many previous states of the system. This extended DFC (EDFC) scheme achieves stabilization of UPOs with a greater degree of instability [12,13].

The theory of the DFC is rather intricate since it involves nonlinear delay-differential equations. Even linear stability analysis of the delayed feedback systems is difficult. Some general analytical results have been obtained only recently [14–16]. Just *et al.* [14] showed that a finite torsion of the orbits close to the UPO is a necessary condition for the DFC method to work at all. More generally and precisely this topological limitation has been proved by Nakajima [15] and Nakajima and Ueda [16]. They showed that the delayed feed-

back methods fail for any UPO with an odd number of real positive Floquet exponents (FEs). The limitation has been recently eliminated in a new modification of the DFC by introducing into a feedback loop an additional unstable degree of freedom that changes the total number of unstable torsion-free modes to an even number [17].

Several numerical methods for the linear stability analysis of time-delayed feedback systems have been developed. The main difficulty of this analysis is related to the fact that periodic solutions of such systems have an infinite number of FEs, though only several FEs with the largest real parts are relevant for stability properties. The most straightforward method for evaluating several largest FEs is described in Ref. [12]. It adapts the usual procedure of estimating the Lyapunov exponents of strange attractors [18]. This method requires a numerical integration of the variational system of delay-differential equations. Bleich and Socolar [13] devised an elegant method to obtain the stability domain of the system under EDFC in which the delay terms in variational equations are eliminated due to the Floquet theorem and the explicit integration of time-delay equations is avoided. Unfortunately, this method does not define the values of the FEs inside the stability domain and is unsuitable for optimization problems.

An approximate analytical method for estimating the FEs of time-delayed feedback systems has been developed in Refs. [14,19]. Here as well as in Ref. [13] the delay terms in variational equations are eliminated and the Floquet problem is reduced to a system of ordinary differential equations. However, the FEs of the reduced system depend on a parameter that is a function of the unknown FEs themselves. In Refs. [14,19] the problem is solved on the assumption that the FE of the reduced system depends linearly on the parameter. This method gives a better insight into the mechanism of the DFC and leads to reasonable qualitative results. In this paper, we use a similar approach but do not employ the above linear approximation and show how to obtain the exact results. Here we do not consider the problem of stabilizing torsion-free orbits and restrict ourselves to the UPOs that are originated from a flip bifurcation.

―――――
*Electronic address: pyragas@kes0.pfi.lt

The rest of the paper is organized as follows. In Sec. II, we consider the EDFC versus the proportional feedback control (PFC) and derive the transcendental equation relating the Floquet spectra of these two control methods. In Sec. III, we suppose that the FE for the PFC depends linearly on the control gain and derive the main stability properties of the EDFC. The case of nonlinear dependence is considered for the specific examples of the Rössler and Duffing systems in Secs. IV and V, respectively. For these examples we discuss the problem of optimizing the parameters of the delayed feedback controller. The paper is finished with conclusions presented in Sec. VI.

II. PROPORTIONAL VERSUS TIME-DELAYED FEEDBACK

Consider a dynamical system described by ordinary differential equations

$$\dot{\boldsymbol{x}} = \boldsymbol{f}(\boldsymbol{x}, p, t), \tag{1}$$

where the vector $\boldsymbol{x} \in \mathbb{R}^m$ defines the dynamical variables and p is a scalar parameter available for an external adjustment. We imagine that a scalar variable

$$y(t) = g(\boldsymbol{x}(t)) \tag{2}$$

that is a function of dynamic variables $\boldsymbol{x}(t)$ can be measured as the system output. Let us suppose that at $p=0$ the system has an UPO $\boldsymbol{x}_0(t)$ that satisfies $\dot{\boldsymbol{x}}_0 = \boldsymbol{f}(\boldsymbol{x}_0, 0, t)$ and $\boldsymbol{x}_0(t+T) = \boldsymbol{x}_0(t)$, where T is the period of the UPO. Here the value of the parameter p is fixed to zero without a loss of generality. To stabilize the UPO we consider two continuous time feedback techniques, the PFC and the DFC, both introduced in Ref. [3].

The PFC uses the periodic reference signal

$$y_0(t) = g(\boldsymbol{x}_0(t)) \tag{3}$$

that corresponds to the system output if it would move along the desired UPO. For chaotic systems, this periodic signal can be reconstructed [3] from the chaotic output $y(t)$ by using the standard methods for extracting UPOs from chaotic time series data [20]. The control is achieved via adjusting the system parameter by a proportional feedback,

$$p(t) = G[y_0(t) - y(t)], \tag{4}$$

where G is the control gain. If the stabilization is successful the feedback perturbation $p(t)$ vanishes. The experimental implementation of this method is difficult since it is not simply to reconstruct the UPO from experimental data.

More convenient for experimental implementation is the DFC method, which can be derived from the PFC by replacing the periodic reference signal $y_0(t)$ with the delayed output signal $y(t-T)$ [3]:

$$p(t) = K[y(t-T) - y(t)]. \tag{5}$$

Here we exchanged the notation of the feedback gain for K to differ it from that of the proportional feedback. The de-

layed feedback perturbation (5) also vanishes provided the desired UPO is stabilized. The DFC uses the delayed output $y(t-T)$ as the reference signal and the necessity of the UPO reconstruction is avoided. This feature determines the main advantage of the DFC over the PFC.

Hereafter, we consider a more general (extended) version of the delayed feedback control, the EDFC, in which a sum of states at integer multiples in the past is used [11]:

$$p(t) = K\left[(1-R)\sum_{n=1}^{\infty} R^{n-1} y(t-nT) - y(t)\right]. \tag{6}$$

The sum represents a geometric series with the parameter $|R| < 1$ that determines the relative importance of past differences. For $R=0$ the EDFC transforms to the original DFC. The extended method is superior to the original in that it can stabilize UPOs of higher periods and with larger FEs. For experimental implementation, it is important that the infinite sum in Eq. (6) can be generated using only a single time-delay element in the feedback loop.

The success of the above methods can be predicted by a linear stability analysis of the desired orbit. For the PFC method, the small deviations from the UPO $\delta\boldsymbol{x}(t) = \boldsymbol{x}(t) - \boldsymbol{x}_0(t)$ are described by the variational equation

$$\dot{\delta\boldsymbol{x}} = [A(t) + GB(t)]\delta\boldsymbol{x}, \tag{7}$$

where $A(t) = A(t+T)$ and $B(t) = B(t+T)$ are both T-periodic $m \times m$ matrices,

$$A(t) = D_1 \boldsymbol{f}(\boldsymbol{x}_0(t), 0, t), \tag{8a}$$

$$B(t) = D_2 \boldsymbol{f}(\boldsymbol{x}_0(t), 0, t) \otimes D g(\boldsymbol{x}_0(t)). \tag{8b}$$

Here D_1 (D_2) denotes the vector (scalar) derivative with respect to the first (second) argument. The matrix $A(t)$ defines the stability properties of the UPO of the free system and $B(t)$ is the control matrix that contains all the details on the coupling of the control force.

Solutions of Eq. (7) can be decomposed into eigenfunctions according to the Floquet theory,

$$\delta\boldsymbol{x} = \exp(\Lambda t)\boldsymbol{u}(t), \quad \boldsymbol{u}(t) = \boldsymbol{u}(t+T), \tag{9}$$

where Λ is the FE. The spectrum of the FEs can be obtained with the help of the fundamental $m \times m$ matrix $\Phi(G, t)$ that is defined by the equalities

$$\dot{\Phi}(G, t) = [A(t) + GB(t)]\Phi(G, t), \quad \Phi(G, 0) = I. \tag{10}$$

For any initial condition $\boldsymbol{x}_{in}$, the solution of Eq. (7) can be expressed with this matrix, $\boldsymbol{x}(t) = \Phi(G, t)\boldsymbol{x}_{in}$. Combining this equality with Eq. (9), one obtains the system $[\Phi(G, T) - \exp(\lambda T)I]\boldsymbol{x}_{in} = 0$ that yields the desired eigensolutions. The characteristic equation for the FEs reads

$$\det[\Phi(G, T) - \exp(\Lambda T)I] = 0. \tag{11}$$

It defines m FEs Λ_j [or Floquet multipliers $\mu_j = \exp(\Lambda_j T)$], $j = 1, \ldots, m$ that are the functions of the control gain G:

$$\Lambda_j = F_j(G), \quad j = 1, \ldots, m. \tag{12}$$

The values $F_j(0)$ are the FEs of the free system. By assumption, at least one FE of the free UPO has a positive real part. The PFC is successful if the real parts of all eigenvalues are negative, Re $F_j(G) < 0$, $j = 1, \ldots, m$ in some interval of the parameter G.

Consider next the stability problem for the EDFC. The variational equation in this case reads

$$\delta\dot{x} = A(t)\delta x(t) + KB(t)$$
$$\times \left[(1-R)\sum_{n=1}^{\infty} R^{n-1} \delta x(t-nT) - \delta x(t) \right]. \tag{13}$$

The delay terms can be eliminated due to Eq. (9), $\delta x(t - nT) = \exp(-n\Lambda T)\delta x(t)$. As a result the problem reduces to the system of ordinary differential equations similar to Eq. (7),

$$\delta\dot{x} = [A(t) + KH(\Lambda)B(t)]\delta x, \tag{14}$$

where

$$H(\Lambda) = \frac{1 - \exp(-\Lambda T)}{1 - R\exp(-\Lambda T)} \tag{15}$$

is the transfer function of the extended delayed feedback controller. Equations (7) and (14) have the same structure defined by the matrices $A(t)$ and $B(t)$ and differ only by the value of the control gain. The equations become identical if we substitute $G = KH(\Lambda)$. The price one has to pay for the elimination of the delay terms is that the characteristic equation defining the FEs of the EDFC depends on the FEs itself:

$$\det[\Phi(KH(\Lambda), T) - \exp(\Lambda T)I] = 0. \tag{16}$$

Nevertheless, we can take advantage of the linear stability analysis for the PFC in order to predict the stability of the system controlled by time-delayed feedback. Suppose that the functions $F_j(G)$ defining the FEs for the PFC are known. Then the FEs of the UPO controlled by time-delayed feedback can be obtained through solution of the transcendental equations,

$$\Lambda = F_j(KH(\Lambda)), \quad j = 1, \ldots, m. \tag{17}$$

Though a similar reduction of the EDFC variational equation has been considered previously (cf. Refs. [13,14,19]), here we emphasize the physical meaning of the functions $F_j(G)$, namely, these functions describe the dependence of the Floquet exponents on the control gain in the case of the PFC.

In the general case, the analysis of the transcendental equations (17) is not a simple task due to several reasons. First, the analytical expressions of the functions $F_j(G)$ are usually unknown; they can be evaluated only numerically. Second, each FE of the free system $F_j(0)$ yields an infinite number of distinct FEs at $K \neq 0$; different eigenvalue branches that originate from different exponents of the free system may hybridize or cross so that the branches originat-

ing from initially stable FEs may become dominant in some intervals of the parameter K [19]. Third, the functions F_j in the proportional feedback technique are defined for the real-valued argument G; however, we may need a knowledge of these functions for the complex values of the argument $KH(\Lambda)$ when considering the solutions of Eqs. (17).

In spite of the possible occurrence of the above difficulties, there are many specific, practically important problems for which the most important information on the EDFC performance can be simply extracted from Eqs. (15) and (17). Such problems cover low-dimensional systems whose UPOs arise from a period-doubling bifurcation.

In what follows we concentrate on the special type of free orbits, namely, those that flip their neighborhood during one turn. More specifically, we consider UPOs whose leading Floquet multiplier is real and negative so that the corresponding FE obeys Im $F_1(0) = \pi/T$. It means that the FE is placed on the boundary of the "Brillouin zone." Such FEs are likely to remain on the boundary under various perturbations and hence the condition Im $F_1(G) = \pi/T$ holds in some finite interval of the control gain $G \in [G_{min}, G_{max}]$, $G_{min} < 0$, $G_{max} > 0$. Subsequently we shall see that the main properties of the EDFC can be extracted from the function Re $F_1(G)$, with the argument G varying in the above interval.

Let us introduce the dimensionless function

$$\phi(G) = F_1(G)T - i\pi \tag{18}$$

that describes the dependence of the real part of the leading FE on the control gain G for the PFC and denote by

$$\lambda = \Lambda T - i\pi \tag{19}$$

the dimensionless FE of the EDFC shifted by the amount π along the complex axes. Then from Eqs. (15) and (17) we derive

$$\lambda = \phi(G), \tag{20a}$$

$$K = G\frac{1 + R\exp[-\phi(G)]}{1 + \exp[-\phi(G)]}. \tag{20b}$$

These equations define the parametric dependence λ versus K for the EDFC. Here G is treated as an independent real-valued parameter. We suppose that it varies in the interval $[G_{min}, G_{max}]$ so that the leading exponent $F_1(G)$ associated with the PFC remains on the boundary of the "Brillouin zone." Then the variables λ, K, and the function ϕ are all real valued.

To demonstrate the benefit of Eqs. (20) let us derive the stability threshold of the UPO controlled by the extended time-delayed feedback. The stability of the periodic orbit is changed when λ reverses the sign. From Eq. (20a) it follows that the function $\phi(G)$ has to vanish for some value $G = G_1$, $\phi(G_1) = 0$. The value of the control gain G_1 is nothing but the stability threshold of the UPO controlled by the proportional feedback. Then from Eq. (20b) one obtains the stability threshold
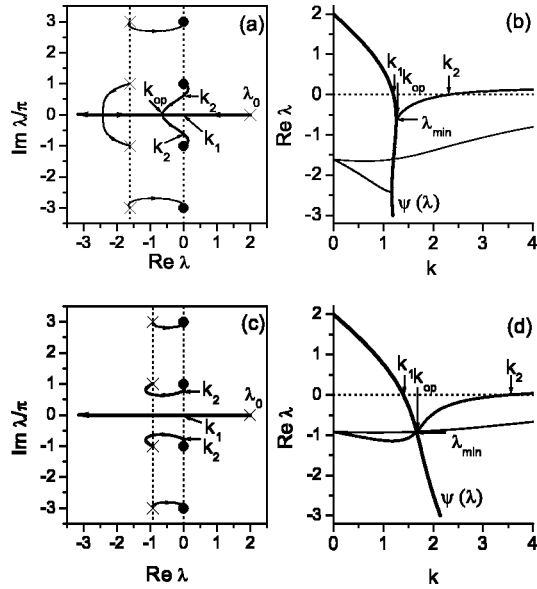
FIG. 1. Root loci of Eq. (23) as k varies from 0 to ∞ and dependence Re λ vs k for $\lambda_0 = 2$ and two different values of the parameter R: (a) and (b) $R = 0.2 < R^*$, (c) and (d) $R = 0.4 > R^*$. The crosses and circles denote the location of roots at $k = 0$ and $k \rightarrow \infty$, respectively. Thick solid lines in (b) and (c) symbolized by $\psi(\lambda)$ are the dependences $k = \psi(\lambda)$ for real λ.

$$K_1 = G_1(1+R)/2 \qquad (21)$$

for the extended time-delayed feedback. In Secs. IV and V we shall demonstrate how to derive other properties of the EDFC by using the specific examples of chaotic systems, but first we consider general features of the EDFC for a simple example in which a linear approximation of the function $\phi(G)$ is assumed.

III. PROPERTIES OF THE EDFC: SIMPLE EXAMPLE

To demonstrate the main properties of the EDFC let us suppose that the function $\phi(G)$ defining the FE for the proportional feedback depends linearly on the control gain G (cf. Refs. [14,19]),

$$\phi(G) = \lambda_0(1 - G/G_1). \qquad (22)$$

Here λ_0 denotes the dimensionless FE of the free system and G_1 is the stability threshold of the UPO controlled by proportional feedback. Substituting approximation (22) into Eq. (20) one derives the characteristic equation

$$k = (\lambda_0 - \lambda)\frac{1 + R\exp(-\lambda)}{1 + \exp(-\lambda)} \equiv \psi(\lambda), \qquad (23)$$

defining the FEs for the EDFC. Here $k = K\lambda_0/G_1$ is the renormalized control gain of the extended time-delayed feedback. The periodic orbit is stable if all the roots of Eq. (23) are in the left half-plane Re $\lambda < 0$. The characteristic root-locus diagrams and the dependence Re λ versus k for two different values of the parameter R are shown in Fig. 1. The zeros and poles of $\psi(\lambda)$ function define the value of roots at

$k = 0$ and $k \rightarrow \infty$, respectively. For $k = 0$ (an open loop system), there is a real-valued root $\lambda = \lambda_0 > 0$ that corresponds to the FE of the free UPO and an infinite number of the complex roots $\lambda = \ln R + i\pi n$, $n = \pm 1, \pm 3, \ldots$ in the left half-plane associated with the extended delayed feedback controller. For $k \rightarrow \infty$, the roots tend to the locations $\lambda = i\pi n$, $n = \pm 1, \pm 3, \ldots$ determined by the poles of $\psi(\lambda)$ function. For intermediate values of K, the roots can evolve by two different scenarios depending on the value of the parameter R.

If R is small enough ($R < R^*$) the conjugate pair of the controller's roots $\lambda = \ln R \pm i\pi$ collide on the real axes [Fig. 1(a)]. After collision, one of these roots moves along the real axes towards $-\infty$, and another approaches the FE of the UPO, then collides with this FE at $k = k_{op}$ and pass to the complex plane. Afterwards this pair of complex conjugate roots moves towards the points $\pm i\pi$. At $k = k_2$ they cross into the right half plane. In the interval $k_1 < k < k_2$ all roots of Eq. (23) are in the left half plane and the UPO controlled by the extended time-delayed feedback is stable. The left boundary of the stability domain satisfies Eq. (21). For the renormalized value of the control gain it reads

$$k_1 = \lambda_0(1+R)/2. \qquad (24)$$

An explicit analytical expression for the right boundary k_2 is unavailable. Inside the stability domain there is an optimal value of the control gain $k = k_{op}$ that for the fixed R provides the minimal value λ_{min} for the real part of the leading FE [Fig. 1(b)]. To obtain the values k_{op} and λ_{min} it suffices to examine the properties of the function $\psi(\lambda)$ for the real values of the argument λ. The values k_{op} and λ_{min} are conditioned by the maximum of this function and satisfy the equalities

$$\psi'(\lambda_{min}) = 0, \quad k_{op} = \psi(\lambda_{min}). \qquad (25)$$

The above scenario is valid when the function $\psi(\lambda)$ possesses the maximum. The maximum disappears at $R = R^*$, when it collides with the minimum of this function so that the conditions $\psi'(\lambda) = 0$ and $\psi''(\lambda) = 0$ are fulfilled. For $\lambda_0 = 2$, these conditions yield $R^* \approx 0.255$.

Now we consider an evolution of roots for $R > R^*$ [Figs. 1(c,d)]. In this case the modes related to the controller and the UPO evolve independently from each other. The FE of the UPO moves along the real axes towards $-\infty$ without hybridizing with the modes of the controller. As done previously, the left boundary k_1 of the stability domain is determined by Eq. (24). The right boundary k_2 is conditioned by the controller mode associated with the roots $\lambda = \ln R \pm i\pi$ at $k = 0$ that move towards $\lambda = \pm i\pi$ for $k \rightarrow \infty$. The optimal value k_{op} is defined by a simple intersection of the real part of this mode with the mode related to the UPO.

Stability domains of the periodic orbit in the plane of parameters (k, R) are shown in Fig. 2(a). The left boundary of this domain is the straight line defined by Eq. (24). The right boundary is determined by parametric equations
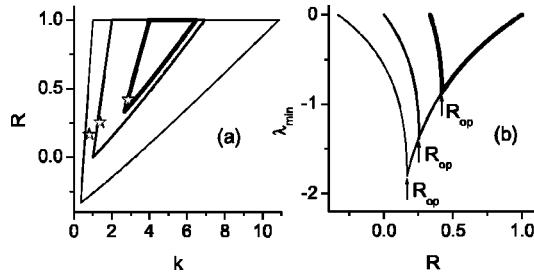
FIG. 2. (a) Stability domains of Eq. (23) in (k,R) plane and (b) dependence λ_{min} vs R for different values of λ_0: 1, 2, and 4 (increasing line thickness corresponds to increasing values of λ_0). The stars inside the stability domains denote the optimal values (k_{op}, R_{op}).

$$k_2 = \frac{\lambda_0^2 + s^2}{\lambda_0 + s \cot(s/2)}, \quad R = \frac{\lambda_0 - s \cot(s/2)}{\lambda_0 + s \cot(s/2)}, \quad (26)$$

with the parameter s varying in the interval $[0,\pi]$. As is seen from the figure, the stability domain is smaller for the UPOs with a larger FE λ_0. Figure 2(b) shows the optimal properties of the EDFC, namely, the dependence λ_{min} versus R, where λ_{min} is the value of the leading Floquet mode evaluated at $k = k_{op}$. This dependence possesses a minimum at $R = R_{op} = R^*$. Thus for any given λ_0 there exists an optimal value of the parameter $R = R_{op}$ that at $k = k_{op}$ provides the fastest convergence of nearby trajectories to the desired periodic orbit. For $R > R_{op}$, the performance of the EDFC is adversely affected with the increase in R since for R close to 1 the modes of the controller are damped out very slowly, $\text{Re}\lambda = \ln R$.

In this section we used an explicit analytical expression for the function $\phi(G)$ when analyzing the stability properties of the UPO controlled by the extended time-delayed feedback. In the next sections we consider a situation where the function $\phi(G)$ is available only numerically and only for real values of the parameter G. We show that in this case the main stability characteristics of the system controlled by time-delayed feedback can be derived as well.

IV. RÖSSLER SYSTEM

Let us consider the problem of stabilizing the period-one UPO of the Rössler system [21]:

$$\begin{pmatrix} \dot{x}_1 \\ \dot{x}_2 \\ \dot{x}_3 \end{pmatrix} = \begin{pmatrix} -x_2 - x_3 \\ x_1 + ax_2 \\ b + (x_1 - c)x_3 \end{pmatrix} + p(t) \begin{pmatrix} 0 \\ 1 \\ 0 \end{pmatrix}. \quad (27)$$

Here we suppose that the feedback perturbation $p(t)$ is applied only to the second equation of the Rössler system and the dynamic variable x_2 is an observable available at the system output, i.e., $y(t) = g(\mathbf{x}(t)) = x_2(t)$.

For parameter values $a = 0.2$, $b = 0.2$, and $c = 5.7$, the free $[p(t) \equiv 0]$ Rössler system exhibits chaotic behavior. An approximate period of the period-one UPO $\mathbf{x}_0(t) = \mathbf{x}_0(t+T)$ embedded in chaotic attractor is $T \approx 5.88$. By linearizing Eq.
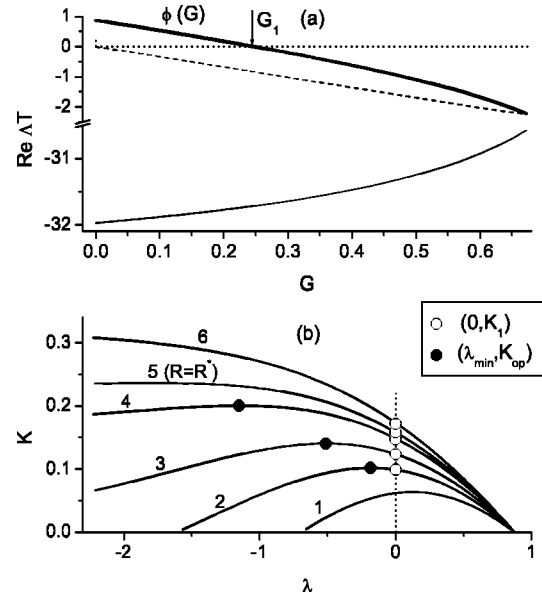

FIG. 3. (a) FEs of the Rössler system under PFC as a function of the control gain G. Thick solid, thin broken, and thin solid lines represent the functions $\Lambda_1 T - i\pi$, $\Lambda_2 T$ (zero exponent), and $\Lambda_3 T - i\pi$, respectively. (b) Parametric dependence K vs λ defined by Eqs. (20) for the EDFC. The numbers mark the curves with different values of the parameter R: (1) -0.5, (2) -0.2, (3) 0, (4) 0.2, (5) 0.28, (6) 0.4. Solid dots show the maxima of the curves and open circles indicate their intersections with the line $\lambda = 0$.

(27) around the UPO, one obtains explicit expressions for the matrices $A(t)$ and $B(t)$ defined in Eq. (8):

$$A(t) = \begin{pmatrix} 0 & -1 & -1 \\ 1 & a & 0 \\ x_3^0(t) & 0 & x_1^0(t) - c \end{pmatrix} \quad (28)$$

and $B = \text{diag}(0, -1, 0)$. Here $x_j^0(t)$ denotes the j component of the UPO.

First we consider the system (27) controlled by proportional feedback, when the perturbation $p(t)$ is defined by Eq. (4). By solving Eqs. (10) and (11) we obtain three FEs, Λ_1, Λ_2, and Λ_3 as a function of the control gain G. The real parts of these functions are presented in Fig. 3(a). The values of the FEs of the free ($G = 0$) UPO are $\Lambda_1 T = 0.876 + i\pi$, $\Lambda_2 T = 0$, $\Lambda_3 T = -31.974 + i\pi$. Thus the first and the third FEs are located on the boundary of the "Brillouin zone." The second, zero FE, is related to the translational symmetry that is general for any autonomous system. The dependence of the FEs on the control gain G is rather complex if it would be considered in a large interval of the parameter G. In Fig. 3(a), we restricted ourselves to a small interval of the parameter $G \in [0, 0.67]$ in which all FEs do not change their imaginary parts, i.e., the FEs Λ_1 and Λ_3 remain on the boundary of the "Brillouin zone," $\text{Im} \Lambda_1 T = i\pi$, $\text{Im} \Lambda_3 T = i\pi$, and Λ_2 remains real valued, $\text{Im} \Lambda_2 T = 0$ for any G in the above interval. An information on the behavior of the leading FE Λ_1 or, more precisely, of the real-valued function $\phi(G) = \Lambda_1 T$

$-i\pi$ in this interval, will suffice to derive the main stability properties of the system controlled by time-delayed feedback.

The main information on the EDFC performance can be gained from parametric Eqs. (20). They make possible a simple reconstruction of the relevant Floquet branch in the (K,λ) plane. This Floquet branch is shown in Fig. 3(b) for different values of the parameter R. Let us denote the dependence K versus λ corresponding to this branch by a function ψ, $K=\psi(\lambda)$. Formally, an explicit expression for this function can be written in the form

$$\psi(\lambda)=\phi^{-1}(\lambda)\frac{1+R\exp(-\lambda)}{1+\exp(-\lambda)}, \quad (29)$$

where ϕ^{-1} denotes the inverse function of $\phi(G)$. More convenient for graphical representation of this dependence is, of course, the parametric form (20). The EDFC will be successful if the maximum of this function is located in the region $\lambda<0$. Then the maximum defines the minimal value of the leading FE λ_{min} for the EDFC and $K_{op}=\psi(\lambda_{min})$ is the optimal value of the control gain at which the fastest convergence of the nearby trajectories to the desired orbit is attained. From Fig. 3(b) it is evident, that the delayed feedback controller should gain in performance through increase of the parameter R since the maximum of the $\psi(\lambda)$ function moves to the left. At $R=R^{*}\approx0.28$ the maximum disappears. For $R>R^{*}$, it is difficult to predict the optimal characteristics of the EDFC. In Sec. III we have established that in this case the value λ_{min} is determined by the intersection of different Floquet branches.

The left boundary of the stability domain is defined by equality $K_{1}=\psi(0)$ [Fig. 3(b)] or alternatively by Eq. (21), $K_{1}=G_{1}(1+R)/2$. This relationship between the stability thresholds of the periodic orbit controlled by the PFC and the EDFC is rather universal; it is valid for systems whose leading FE of the UPO is placed on the boundary of the "Brillouin zone." It is interesting to note that the stability threshold for the original DFC ($R=0$) is equal to the half of the threshold in the case of the PFC, $K_{1}=G_{1}/2$.

An evaluation of the right boundary K_{2} of the stability domain is a more intricate problem. Nevertheless, for the parameter $R<R^{*}$ it can be successfully solved by means of an analytical continuation of the function $\psi(\lambda)$ on the complex region. For this purpose we expand the function $\psi(\lambda)$ at the point $\lambda=\lambda_{min}$ into power series

$$\psi(\lambda)=K_{op}+\sum_{n=2}^{N+1}\alpha_{n}(\lambda-\lambda_{min})^{n}. \quad (30)$$

The coefficients α_{n} we evaluate numerically by the least-squares fitting. In this procedure we use a knowledge of numerical values of the function $\psi(\lambda_{m})$, $m=1,\dots,M$ in $M>N$ points placed on the real axes and solve a corresponding system of N linear equations. To extend the Floquet branch to the region $K>K_{op}$ we have to solve the equation $K=\psi(\lambda)$ for the complex argument λ. Substituting $\lambda-\lambda_{min}=r\exp(i\varphi)$ into Eq. (30) we obtain
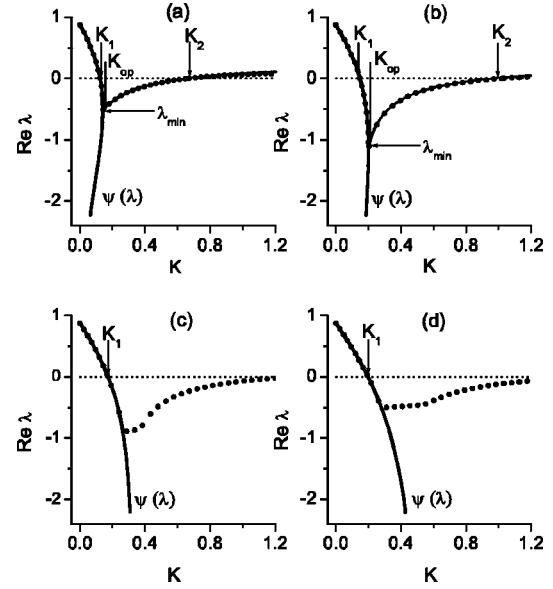

FIG. 4. Leading FEs of the Rössler system under EDFC as a function of the control gain K for different values of the parameter R: (a) 0.1, (b) 0.2, (c) 0.4, (d) 0.6. Thick solid lines symbolized by $\psi(\lambda)$ show the dependence $K=\psi(\lambda)$ for real λ. Solid lines in the region $K>K_{op}$ are defined from Eqs. (31). The number of terms in series (30) is $N=15$. Solid black dots denote the "exact" solutions obtained from complete system of Eqs. (10), (15), (16).

$$\sum_{n=2}^{N+1}\alpha_{n}r^{n}\sin n\varphi=0, \quad (31a)$$

$$K=K_{op}+\sum_{n=2}^{N+1}\alpha_{n}r^{n}\cos n\varphi, \quad (31b)$$

$$\operatorname{Re}\lambda=\lambda_{min}+r\cos\varphi, \quad (31c)$$

$$\operatorname{Im}\lambda=r\sin\varphi. \quad (31d)$$

Let us suppose that r is an independent parameter. By solving Eq. (31a) we can determine φ as a function of r, $\varphi=\varphi(r)$. Then Eqs. (31b),(31c) and (31b),(31d) define the parametric dependences $\operatorname{Re}\lambda$ versus K and $\operatorname{Im}\lambda$ versus K, respectively.

Figure 4 shows the dependence of the leading FEs on the control gain K for the EDFC. The thick solid line represents the most important Floquet branch that conditions the main stability properties of the system. It is described by the function $K=\psi(\lambda)$ with the real argument λ. Note that the same function has been depicted in Fig. 3(b) for inverted axes. For $R<R^{*}$, this branch originates an additional sub-branch, which starts at the point (K_{op},λ_{min}) and spreads to the region $K>K_{op}$. The sub-branch is described by Eqs. (31) that results from an analytical continuation of the function $\psi(\lambda)$ on the complex plane. This sub-branch is leading in the region $K>K_{op}$ and its intersections with the line $\lambda=0$ define the right boundary K_{2} of the stability domain. In Figs. 4(a,b) the sub-branches are shown by solid lines. As seen from the figures, the Floquet sub-branches obtained by means of an
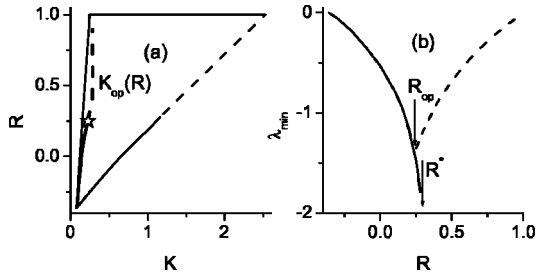
FIG. 5. (a) Stability domain of the period-one UPO of the Rössler system under EDFC. The thick curve inside the domain shows the dependence K_{op} vs R. The star marks the optimal point (K_{op}, R_{op}). (b) Minimal value λ_{min} of the leading FE as a function of the parameter R. In both figures solid and broken lines denote the solutions obtained from Eqs. (20) and Eqs. (10), (15), and (16), respectively.

analytical continuation are in good agreement with the "exact" solutions evaluated from the complete system of Eqs. (10), (15), and (16).

For $R > R^*$, the maximum in the function $\psi(\lambda)$ disappears and the Floquet branch originated from the eigenvalues $\lambda = \ln R \pm i\pi$ of the controller (see Sec. III) becomes dominant in the region $K > K_{op}$. This Floquet branch as well as the intersection point (K_{op}, λ_{min}) are unpredictable via a simple analysis. It can be determined by solving the complete system of Eqs. (10), (15) and (16). In Figs. 4(c,d) these solutions are shown by dots.

Fig. 5 demonstrates how much of information one can gain via a simple analysis of parametric Eqs. (20). These equations allow us to construct the stability domain in the (K, R) plane almost completely. The most important information on optimal properties of the EDFC can be obtained from these equations as well. The thick curve in the stability domain shows the dependence of optimal value of the control gain K_{op} on the parameter R. The star marks an optimal choice of both parameters (K_{op}, R_{op}), which provide the fastest decay of perturbations. Figure 5(b) shows how the decay rate λ_{min} attained at the optimal value of the control gain K_{op} depends on the parameter R. The left part of this dependence is simply defined by the maximum of the function $\psi(\lambda)$ while the right part is determined by intersection of different Floquet branches and can be evaluated only with the complete system of Eqs. (10), (15), and (16). Unlike the simple model considered in Sec. II here the intersection occurs before the maximum in the function $\psi(\lambda)$ disappears, i.e., at $R = R_{op} < R^*$. Nevertheless, the value R^* gives a good estimate for the optimal value of the parameter R, since R^* is close to R_{op}.

V. DUFFING OSCILLATOR

To justify the universality of the proposed method we demonstrate its suitability for nonautonomous systems. As a typical example of such a system we consider the Duffing oscillator

$$\begin{pmatrix} \dot{x}_1 \\ \dot{x}_2 \end{pmatrix} = \begin{pmatrix} x_2 \\ x_1 - x_1^3 - \gamma x_2 + a\sin\omega t \end{pmatrix} + p(t)\begin{pmatrix} 0 \\ 1 \end{pmatrix}. \quad (32)$$
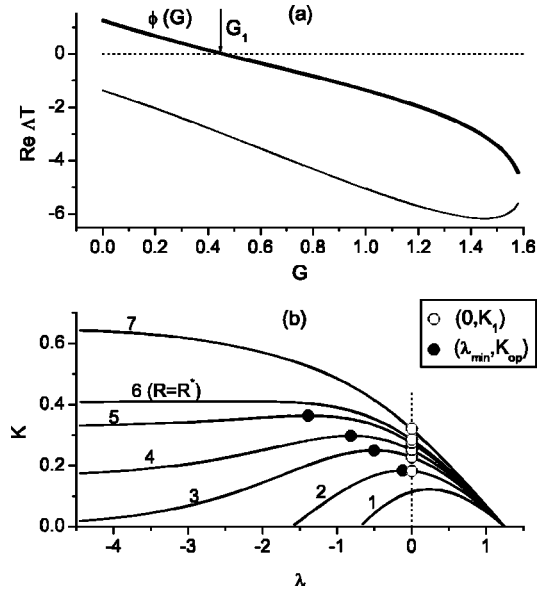

FIG. 6. (a) FEs of the Duffing oscillator under PFC, as a function of the control gain G. Thick and thin solid lines denote the function $\Lambda_1 T - i\pi$ and $\Lambda_2 T - i\pi$, respectively. (b) The dependence K vs λ for the EDFC defined by parametric Eqs. (20). The numbers mark the curves with different values of the parameter R: (1) -0.5, (2) -0.2, (3) 0, (4) 0.1, (5) 0.2, (6) 0.25, (7) 0.4.

Here γ is the damping coefficient of the oscillator. The parameters a and ω are the amplitude and the frequency of the external force, respectively. We assume that the speed x_2 of the oscillator is the observable, i.e., $y(t) = g(\mathbf{x}(t)) = x_2$ and the feedback force $p(t)$ is applied to the second equation of the system (32). We fix the values of parameters $\gamma = 0.02$, $a = 2.5$, $\omega = 1$ so that the free $[p(t) \equiv 0]$ system is in chaotic regime. The period of the period-one UPO embedded in chaotic attractor coincides with the period of the external force $T = 2\pi/\omega = 2\pi$. Linearization of Eq. (32) around the UPO yields the matrices $A(t)$ and $B(t)$ of the form

$$A(t) = \begin{pmatrix} 0 & 1 \\ 1 - 3[x_1^0(t)]^2 & -\gamma \end{pmatrix}, \quad B = \begin{pmatrix} 0 & 0 \\ 0 & -1 \end{pmatrix}. \quad (33)$$

First we analyze the Duffing oscillator under proportional feedback defined by Eq. (4). This system is nonautonomous and does not have the zero FE. By solving Eqs. (10) and (11) we obtain two FEs Λ_1 and Λ_2 as a function of the control gain G. The real parts of these functions are presented in Fig. 6(a). Both FEs of the free ($G = 0$) UPO are located on the boundary of the "Brillouin zone," $\Lambda_1 T = 1.248 + i\pi$, $\Lambda_2 T = 0$, $\Lambda_2 T = -1.373 + i\pi$. As before, we restrict ourselves with a small interval of the parameter $G \in [0, 1.6]$ in which both FEs remain on the boundary.

As was in the previous example, the main properties of the system controlled by time-delayed feedback can be obtained from parametric Eqs. (20). Figure 6(b) shows the dependence $K = \psi(\lambda)$ for different values of the parameter R. For the fixed value of R, the maximum of this function defines the optimal control gain $K_{op} = \psi(\lambda_{min})$. The maximum
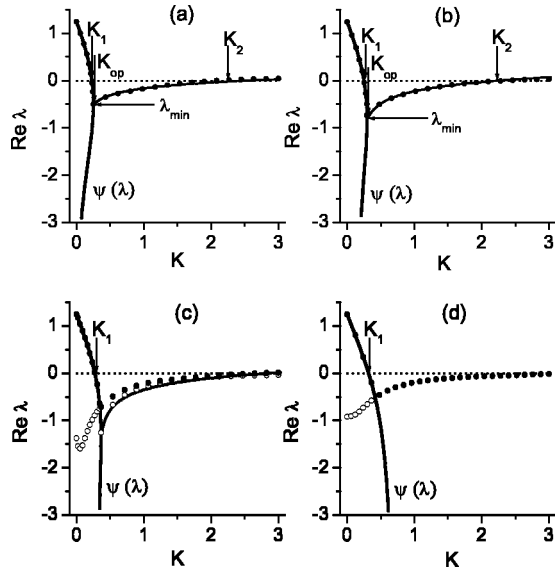
FIG. 7. The same as in the Fig. 4 but for the Duffing oscillator. The values of the parameter R are (a) 0, (b) 0.1, (c) 0.2, (d) 0.4. Open circles denote the second largest FE obtained from complete system of Eqs. (10), (15), and (16).

FIG. 8. The same as in Fig. 5 but for the Duffing oscillator.

disappears at $R = R^* \approx 0.25$. The left boundary of the stability domain is $K_1 = \psi(0) = G_1(1+R)/2$, as previously.

Figure 7 shows the results of analytical continuation of the relevant Floquet branch on the region $K > K_{op}$. The continuation is performed via Eqs. (31). For small values of the parameter R [Fig. 7(a,b)], a good quantitative agreement with the ''exact'' result obtained from complete system of Eqs. (10), (15), and (16) is attained. For $R = 0.2 < R^*$, the Floquet mode associated with the controller becomes dominant in the region $K > K_{op}$. In this case the analytical continuation predicts correctly the second largest FE.

Again, as in the previous example, a simple analysis of parametric Eq. (20) allows us to construct the stability domain in the (K,R) plane almost completely [Fig. 8(a)] and to obtain the most important information on the optimal properties of the delayed feedback controller [Fig. 8(b)].

VI. CONCLUSIONS

In this paper, we have demonstrated how to utilize the relationship between the Floquet spectra of the system controlled by proportional and time-delayed feedback in order to obta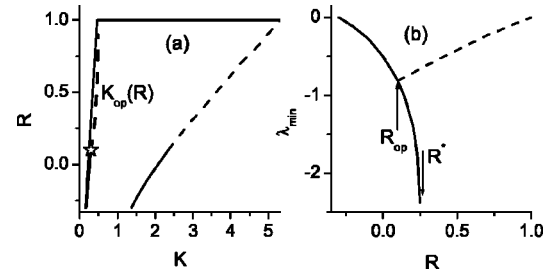in the main stability properties of the system controlled by time-delayed feedback. Our consideration is restricted to low-dimensional systems whose unstable periodic orbits originate from a period doubling bifurcation. These orbits flip their neighborhood during one turn so that the leading Floquet exponent is placed on the boundary of the ''Brillouin zone.'' Knowing the dependence of this exponent on the control gain for the proportional feedback control one can simply construct the relevant Floquet branch for the case of time-delayed feedback control. As a result the stability domain of the orbit controlled by time-delayed feedback as well as optimal properties of the delayed feedback controller can be evaluated without an explicit integration of time-delay equations.

The proposed algorithm gives a better insight into how the Floquet spectrum of periodic orbits controlled by time-delayed feedback is formed. We believe that the ideas of this approach will be useful for further development of time-delayed feedback control techniques and will stimulate a search for other modifications of the method in order to gain better performance.

Here no consideration has been given to the torsion-free periodic orbits. These orbits can be stabilized with the unstable time-delayed feedback controller proposed recently in Ref. [17]. Stability analysis of such systems can be performed in a similar manner as described in this paper. This problem is currently under investigation and the results will be published elsewhere.

[1] E. Ott, C. Grebogi, and J.A. Yorke, Phys. Rev. Lett. **64**, 1196 (1990).

[2] T. Shinbrot, C. Grebogy, E. Ott, and J.A. Yorke, Nature (London) **363**, 411 (1993); *Handbook of Chaos Control*, edited by H.G. Shuster (Willey-VCH, Weiheim, 1999); S. Boccaletti, C. Grebogi, Y.-C. Lai, H. Mancini, and D. Maza, Phys. Rep. **329**, 103 (2000).

[3] K. Pyragas, Phys. Lett. A **170**, 421 (1992).

[4] K. Pyragas and A. Tamaševičius, Phys. Lett. A **180**, 99 (1993);

A. Kittel, J. Parisi, K. Pyragas, and R. Richter, Z. Naturforsch., A: Phys. Sci. **49**, 843 (1994); D.J. Gauthier, D.W. Sukow, H.M. Concannon, and J.E.S. Socolar, Phys. Rev. E **50**, 2343 (1994).

[5] T. Hikihara and T. Kawagoshi, Phys. Lett. A **211**, 29 (1996); D.J. Christini, V. In, M.L. Spano, W.L. Ditto, and J.J. Collins, Phys. Rev. E **56**, R3749 (1997).

[6] S. Bielawski, D. Derozier, and P. Glorieux, Phys. Rev. E **49**, R971 (1994); W. Lu, D. Yu, and R.G. Harrison, Int. J. Bifur-

cation Chaos Appl. Sci. Eng. **8**, 1769 (1998).

[7] Th. Mausbach, Th. Klinger, A. Piel, A. Atipo, Th. Pierre, and G. Bonhomme, Phys. Lett. A **228**, 373 (1997).

[8] O. Lüthje, S. Wolff, and G. Pfister, Phys. Rev. Lett. **86**, 1745 (2001).

[9] P. Parmananda, R. Madrigal, M. Rivera, L. Nyikos, I.Z. Kiss, and V. Gaspar, Phys. Rev. E **59**, 5266 (1999); A.P.M. Tsui and A.J. Jones, Physica D **135**, 41 (2000).

[10] K. Hall, D.J. Christini, M. Tremblay, J.J. Collins, L. Glass, and J. Billette, Phys. Rev. Lett. **78**, 4518 (1997).

[11] J.E.S. Socolar, D.W. Sukow, and D.J. Gauthier, Phys. Rev. E **50**, 3245 (1994).

[12] K. Pyragas, Phys. Lett. A **206**, 323 (1995).

[13] M.E. Bleich and J.E.S. Socolar, Phys. Lett. A **210**, 87 (1996).

[14] W. Just, T. Bernard, M. Ostheimer, E. Reibold, and H. Benner, Phys. Rev. Lett. **78**, 203 (1997).

[15] H. Nakajima, Phys. Lett. A **232**, 207 (1997).

[16] H. Nakajima and Y. Ueda, Physica D **111**, 143 (1998).

[17] K. Pyragas, Phys. Rev. Lett. **86**, 2265 (2001).

[18] G. Benettin, C. Froeschle, and J.P. Scheidecker, Phys. Rev. A **19**, 2454 (1979); I. Schimada and T. Nagashima, Prog. Theor. Phys. **61**, 1605 (1979).

[19] W. Just, E. Reibold, H. Benner, K. Kacperski, P. Fronczak, and J. Holyst, Phys. Lett. A **254**, 158 (1999); W. Just, E. Reibold, K. Kacperski, P. Fronczak, J.A. Holyst, and H. Benner, Phys. Rev. E **61**, 5045 (2000).

[20] D.P. Lathrop and E.J. Kostelich, Phys. Rev. A **40**, 4028 (1989); P. So, E. Ott, S.J. Schiff, D.T. Kaplan, T. Sauer, and C. Grebogi, Phys. Rev. Lett. **76**, 4705 (1996); P. So, E. Ott, T. Sauer, B.J. Gluckman, C. Grebogi, and S.J. Schiff, Phys. Rev. E **55**, 5398 (1997).

[21] O.E. Rössler, Phys. Lett. A **57**, 397 (1976).